Kinetic and Mechanistic Study with Optically Active, Four-Coordinate Nickel(II) Complexes: Stereoselectivity in Ligand Substitution

Alexander Haus, Michael Raidt, Thomas A. Link,† and Horst Elias*

Institut für Anorganische Chemie, Technische Universität Darmstadt, Petersenstrasse 18, D-64287 Darmstadt, Federal Republic of Germany

Received March 29, 2000

Conventional and rapid scan stopped-flow spectrophotometry as well as polarimetry was used to study the kinetics of ligand substitution in six chiral bis *N*-alkylsalicylaldiminato nickel(II) complexes NiA_2 by different chiral salen-type ligands H_2B, according to $NiA_2 + H_2B \rightarrow NiB + 2HA$, in acetone at 298 K and, partly, at variable temperature. In most cases ligand substitution was found to follow monophasic second-order kinetics, rate $= k \times [NiA_2] \times [H_2B]$. Second-order rate constant k, lying in the range $10^{-2} - 400\ M^{-1}s^{-1}$ at 298 K, was determined for the various combinations of enantiomers in a given system NiA_2/H_2B, namely, *R*-NiA_2/*R*-H_2B, *S*-NiA_2/*R*-H_2B, *R*-NiA_2/*S*-H_2B, and *S*-NiA_2/*S*-H_2B. It was found that ligand substitution is subject to chiral discrimination. The ratio of second-order rate constants, k_{fast}/k_{slow}, with k_{fast} being rate constant k for the faster reacting pair of enantiomers and vice versa, lies in the range 1.0−3.0, depending on the nature of the *N*-alkyl groups in NiA_2 and organic groups attached to the ethylene bridge in the salen ligands H_2B. The rate discrimination factor of 3.0, as obtained for NiA_2 = bis[*N*-dehydroabietylsalicylaldiminato]nickel(II) reacting with the *R*- and with the *S*-enantiomer of H_2B = *N*,*N*′-disalicylidene-1,2-diamino-4-methylpentane, appears to be the highest stereoselectivity reported so far for ligand substitution in nickel(II) complexes. With NiA_2 = *R*- and *S*-bis[*N*-(1-phenylethyl)-5-nitrosalicylaldiminato]nickel(II) and H_2B = *R*- and *S*-*N*,*N*′-disalicylidene-1,2-diamino-4-methylpentane, the kinetics of ligand substitution are biphasic, describing initial adduct formation between NiA_2 and H_2B (equilibrium constant K) and stepwise loss of the two bidentate ligands HA (first-order rate constants k_1 and k_2). The data for K, k_1, and k_2 for one of the combinations of enantiomers were determined at variable temperature, and the corresponding activation parameters are presented.

Introduction

Chiral recognition is a phenomenon of utmost importance for the functioning of biological systems as well as for chemical synthesis. Numerous recent monographs[1] and review articles[2] document the rapidly growing interest in stereoselective synthesis and asymmetric catalysis. Chiral metal complexes, such as the manganese(III) salen complex introduced by Jacobsen and co-workers,[3] play an important role as catalysts for stereoselective reactions. The catalytic function of many transition metal complexes can be described schematically by eqs 1 and 2.

$$ML + S \overset{K_{ad}}{\rightleftharpoons} \{ML,S\} \quad (1)$$

$$\{ML,S\} + \text{reagent} \xrightarrow{k_p} ML + \text{product P} \quad (2)$$

A chiral complex ML equilibrates with a prochiral substrate S to form diastereomeric adducts {ML,S}, which react with an excess of reagent to form stereoselectively the product P. One of the fundamental questions to be raised in the case of such stereoselective reactions concerns the origin of stereoselectivity, which can be thermodynamic (K_{ad}) or kinetic (k_p). Systems which are suited to answer this question are rare. The studies of Halpern and co-workers[4] on the rhodium-catalyzed hydrogenation of prochiral olefins led to a system which allowed the determination of K_{ad} and k_p for both of the diastereomeric adducts {Rh^{I}L,olefin} formed according to eq 1. The results obtained for this system were explained on the basis of the so-called "major/minor" principle, which ascribes the stereoselectivity of the overall reaction to the preference of the one reaction path characterized by a small value of K_{ad} and a high value of k_p.

In contrast to stereoselective electron-transfer reactions of transition metal complexes,[5,6] studies on stereoselective ligand substitution in metal complexes are rare.[7,8] In an earlier contribution[9] we reported on the kinetics of ligand substitution

* To whom correspondence should be addressed. E-mail: Elias@tu-darmstadt.de.

† Institut für Biophysik, Johann Wolfgang Goethe-Universität Frankfurt, Theodor-Stern-Kai 7, Haus 75, D-60590 Frankfurt/Main, Federal Republic of Germany.

(1) *Catalytic Asymmetric Synthesis*; Ojima, I., Ed.; Wiley-VCH: Weinheim, 1993. (b) Noyori, R. *Asymmetric Catalysis in Organic Synthesis*; Wiley: New York, 1995. (c) Atkinson, R. S. *Stereoselective Synthesis*; Wiley: New York, 1995. (d) Nógrádi, M. *Stereoselective Synthesis: A Practical Approach*; VCH: Weinheim, 1995.

(2) Gladysz, J. A.; Boone, B. J. *Angew. Chem., Int. Ed. Engl.* **1997**, *36*, 551. (b) Canali, L.; Sherrington, D. C. *Chem. Soc. Rev.* **1999**, *28*, 85. (c) Ito, Y. N.; Katsuki, T. *Bull. Chem. Soc. Jpn.* **1999**, *72*, 603.

(3) Zhang, W.; Loebach, J. L.; Wilson, S. R.; Jacobsen, E. N. *J. Am. Chem. Soc*. **1990**, *112*, 2801. (b) Zhang, W.; Jacobsen, E. N. *J. Org. Chem.* **1991**, *56*, 2296. (c) Jacobsen, E. N.; Zhang, W.; Güler, M. L. *J. Am. Chem. Soc.* **1991**, *113*, 6703.

(4) Halpern, J. *Pure Appl. Chem.* **1983**, *55*, 99. (b) Landis, C. R.; Halpern, J. *J. Am. Chem. Soc.* **1987**, *109*, 1746.

(5) Bernauer, K. Stereoselective Effects in Electron-Transfer Reactions Involving Synthetic Metal Complexes Metalloproteins. In *Metal Ions in Biological Systems*; Sigel, H., Sigel, A., Eds.; Marcel Dekker: New York and Basel, 1991; Vol. 27, Chapter 8, pp 265−289.

(6) Marusak, R. A.; Sharp, C.; Lappin, A. G. *Inorg. Chem.* **1990**, *29*, 2298. (b) Bernauer, K.; Monzione, M.; Schürmann, P.; Viette, V. *Helv. Chim. Acta* **1990**, *73*, 346. (c) Richardson, F. S.; Metcalf, D. H.; Glover, D. P. *J. Phys. Chem.* **1991**, *95*, 6249. (d) Metcalf, D. H.; Bolender, J. P.; Driver, M. S.; Richardson, F. S. *J. Phys. Chem.* **1993**, *97*, 553. (e) Bernauer, K.; Jauslin, P. *Chimia* **1993**, *47*, 218. (f) Nakajima, K.; Ando, Y.; Inamo, M.; Kojima, M. *Chem. Lett.* **1995**, 1017. (g) Tatehata, A.; Muraida, A. *Chem. Lett.* **1996**, 461.

(7) Kurganov, A. A.; Ponomarewa, T. M.; Lavankov, V. A. *Inorg. Chim. Acta* **1984**, *86*, 145. (b) Kurganov, A. A.; Ponomarewa, T. M.; Lavankov, V. A. *Dokl. Chem. (Engl. Transl.)* **1987**, *293*, 147.

(8) Bernauer, K.; Gilet, M.-F. *Chem. Commun.* **1997**, 1287.

10.1021/ic000339m CCC: $19.00
Published on Web 10/12/2000

in chiral salicylaldiminato complexes NiA_2 by chiral salen-type ligands H_2B in acetone according to eq 3.

$$NiA_2 + H_2B \xrightarrow{k} NiB + 2HA \quad (3)$$

The substitution process was found to be second-order according to eq 4. Chiral discrimination was observed in the sense that second-order rate constants k, as obtained for the various combinations of enantiomers of NiA_2 and H_2B, differed by a factor of 1.4−2.1.

$$\text{rate} = k \times [NiA_2] \times [H_2B] \quad (4)$$

To understand the mechanism of the displacement of the two bidentate ligands in NiA_2 by the tetradentate ligand H_2B, we studied reaction (3) with a variety of specially designed complexes NiA_2 and ligands H_2B at ambient and reduced temperature.[10] The kinetic and spectroscopic results obtained proved that substitution reaction (3) is an associatively controlled process consisting of three clearly distinguishable steps according to reaction sequence (5)−(7). Fast adduct formation, as characterized by equilibrium constant K, is followed by rate-

$$NiA_2 + H_2B \overset{K}{\rightleftharpoons} \{NiA_2,H_2B\} \quad (5)$$

$$\{NiA_2,H_2B\} \xrightarrow{k_1} NiAHB + HA \quad (6)$$

$$NiAHB \xrightarrow{k_2} NiB + HA \quad (7)$$

controlling loss of the first bidentate ligand HA according to eq 6. The loss of the second ligand HA is described by first-order rate constant k_2. For small values of K and the condition $k_2 \gg k_1$, the overall reaction appears to be a second-order process according to rate law (4) with $k = k_1 \times K$.

From the kinetic point of view, reaction sequence (5) and (6) is similar to reaction sequence (1) and (2) in that the rate-controlling step is preceded by fast adduct formation. This similarity led us to study ligand substitution reactions (3) with the enantiomers of specifically selected chiral compounds NiA_2 and H_2B, suited to allow the experimental determination of K and k_1 (and possibly also k_2). The knowledge of these parameters would then shed light on the origin of the stereoselectivity of the overall reaction. Chart I summarizes the chiral complexes **1**−**6** and chiral ligands **I**−**IV** applied for the study of reaction (3) in acetone in the present investigation.

Experimental Section

Chemicals. The solvent acetone (analytical grade, Merck) and the salt $Ni(AcO)_2 \times 4H_2O$ (reagent grade, Merck) were used without further purification; salicylaldehyde (for synthesis, Merck); 2-*tert*-butylphenole (for synthesis, Aldrich); 5-nitrosalicylaldehyde (for synthesis, Merck); d-leucine (>99%, Fluka); L-leucine (> 99%, Merck); L-phenylalanine (>99.5%, Acros); d-phenylalanine (>99%, Acros); (*R*)-(+)-1-(1-naphthyl)ethylamine (>99%, Acros); (*S*)-(−)-1-(1-naphthyl)ethylamine (>99%, Fluka); (*R*)-(+)-2-phenyl-1-propylamine and (*S*)-(−)-2-phenyl-1-propylamine (>99%, Fluka); (*R*)-(+)-1-phenylethylamine and (*S*)-(−)-1-phenylethylamine (>99%, Fluka); (+)-dehydroabietylamine (>95%, for resolution of racemates, Merck).

Diamines. The optically active diamines $H_2N-CH_2-CHR'-NH_2$ (for R′ see Chart 1) applied for the condensation reaction with salicylaldehyde were prepared as described.[11]

Chart 1. Structural Formulas of Chiral Complexes NiA_2 and Chiral Ligands H_2B and Abbreviations

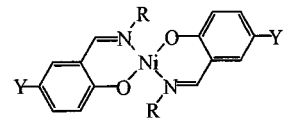

R	Y	Ni(Y-R-sal)$_2$	denotation
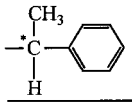	H	Ni(H-PhEt-sal)$_2$	**1**
	NO_2	Ni(NO_2-PhEt-sal)$_2$	**2**
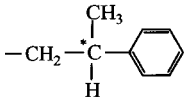	H	Ni(H-PhPr-sal)$_2$	**3**
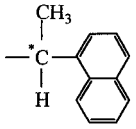	H	Ni(H-NpEt-sal)$_2$	**4**
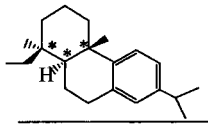	H	Ni(H-Dha-sal)$_2$	**5**
	NO_2	Ni(NO_2-Dha-sal)$_2$	**6**

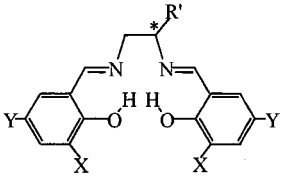

R′	X,Y	H_2(X)(Y)R'salen	denotation
$-CH_3$	H,H	H_2Mesalen	**I**
$-CH_2-CH(CH_3)_2$	H,H	H_2iBusalen	**II**
$-CH_2-CH(CH_3)_2$	*t*-butyl,Cl	H_2[(tBu)(Cl)iBusalen]	**III**
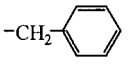	H,H	H_2Bzsalen	**IV**

Ligands H_2B. The optically active Schiff bases **I** (= H_2Mesalen = *N*,*N*′-disalicylidene-1,2-diaminopropane), **II** (= H_2iBusalen = *N*,*N*′-disalicylidene-1,2-diamino-4-methylpentane), **III** (= H_2(tBu)(Cl)-iBusalen = *N*,*N*′-bis(3-*tert*-butyl-5-chlorosalicylidene)-1,2-diamino-4-methylpentane), and **IV** (= H_2Bzsalen = *N*,*N*′-disalicylidene-1,2-diamino-3-phenylpropane) were prepared from salicylaldehyde (and 3-*tert*-butyl-5-chlorosalicylaldehyde, respectively) and the corresponding optically active diamine according to eq 8 in methanol as described.[9,11a] 3-*tert*-Butyl-5-chlorosalicylaldehyde was synthesized as reported by Böttcher et al.[12]

$$2\text{Ph-CHO} + H_2N-CH_2-CHR'-NH_2 \rightarrow \text{Ph-CH=N-CH}_2\text{-CHR'-N=CH-Ph} + 2H_2O \quad (8)$$

The Schiff bases H_2B obtained according to eq 8 are characterized with

(9) Warmuth, R.; Elias, H. *Inorg. Chem.* **1991**, *30*, 5027.
(10) Hoss, H.; Elias, H. *Inorg. Chem.* **1993**, *32*, 317.
(11) Belokon, Y. N.; Yashkina, L. V.; Moscalenko, M. A.; Chesnokov, A. A.; Kublitsky, V. S.; Ikonnikov, N. S.; Orlova, S. A.; Tararov, V. I.; North, M. *Russ. Chem. Bull.* **1997**, *46*, 1936. (b) Brunner, H.; Schmidt, M.; Unger, G.; Schönenberger, H. *Eur. J. Med. Chem.-Chim. Ther.* **1985**, *20*, 509. (c) Brunner, H.; Hankofer, P.; Holzinger, U.; Treittinger, B.; Schönenberger, H. *Eur. J. Med. Chem.* **1990**, *25*, 35.
(12) Böttcher, A.; Elias, H.; Jäger, E.-G.; Langfelderova, H.; Mazur, M.; Müller, L.; Paulus, H.; Pelikan, P.; Rudolph, M.; Valko, M. *Inorg. Chem.* **1993**, *32*, 4131.

Table 1. Visible Absorption Data, Specific Rotation and Circular Dichroism of the Nickel(II) Complexes NiA_2 and NiB and Ligands H_2B at 298 K in Acetone

complex/ligand	λ_{max},nm (ϵ_{max}, l mol^{-1} cm^{-1})	$[\alpha]_D^{20}$, deg mL g^{-1} dm^{-1} [a,b]	λ, nm ($\Delta\epsilon$)
R-(+)-**1**	~400 (sh); 415 (4100); 610 (85)	+1255	~400 (sh); 414 (+5.3); 535 (+0.9); 629 (−0.6)
S-(−)-**1**		−1288	~400 (sh); 414 (−5.2); 535 (−0.9); 628 (+0.6)
R-(+)-**2**	382 (36000); 602 (55); 1075 (25)	+746	366 (+8.1); 478 (−0.23); 539 (+0.3); 616 (−0.4)
S-(−)-**2**		−756	366 (−8.0); ~480 (+); 539 (−0.3); 615 (+0.4)
R-(−)-**3**	415 (4600); 615 (70)	−142	
S-(+)-**3**		+145	
R-(+)-**4**	412 (5000); 615 (100)	+947	
S-(−)-**4**		−921	
(−)-**5**	411 (4060); 603 (70)	−630	
(−)-**6**	385 (34350); 562 (160)	−25	
R-(+)-Ni(*i*Busalen)	411 (7000); 529 (270)	+1500	
S-(−)-Ni(*i*Busalen)		−1510	
R-(+)-Ni[(tBu)(Cl)*i*Busalen]	420 (8600); 550 (320)	+1032	
S-(−)-Ni[(tBu)(Cl)*i*Busalen]		−1004	
R-(+)-Ni(Bzsalen)	413 (8000); 545 (640)	+1431	
S-(−)-Ni(Bzsalen)		−1412	
R-(−)-**I**[c]	410 (65)	−232	
S-(+)-**I**[c]		+214	
R-(−)-**II**	400 (60)	−145	
S-(+)-**II**		+146	
R-(−)-**III**	410 (160)	−132	
S-(+)-**III**		+134	
R-(−)-**IV**	405 (55)	−108	
S-(+)-**IV**		+106	

[a] Limits of error: ±10%. [b] Data refer to 293 K. [c] Data taken from ref 9.

the abbreviations *R*-H_2B and *S*-H_2B to indicate that the diamine applied has the *R*-configuration and *S*-configuraton, respectively.

Complexes NiA_2. The optically active complexes **1** (= Ni(H-PhEt-sal)$_2$ = bis[*N*-(1-phenylethyl)salicylaldiminato]nickel(II)), **2** (= Ni(NO_2-PhEt-sal)$_2$ = bis[*N*-(1-phenylethyl)-5-nitrosalicylaldiminato]nickel(II)), **3** (= Ni(H-PhPr-sal)$_2$ = bis[*N*-(2-phenylpropyl)salicylaldiminato]nickel(II)), **4** (= Ni(H-NpEt-sal)$_2$ = bis[*N*-(1-(1-naphthyl)ethyl)salicylaldiminato]nickel(II)), **5** (= Ni(H-Dha-sal)$_2$ = bis[*N*-dehydroabietylsalicylaldiminato]nickel(II)), and **6** (= Ni(NO_2-Dha-sal)$_2$ = bis[*N*-dehydroabietyl-5-nitrosalicylaldiminato]nickel(II)) were prepared from Ni(sal)$_2\times 2H_2O$ (and Ni(5-NO_2-sal)$_2\times 2H_2O$, respectively; Hsal = salicylaldehyde) and the corresponding optically active amine according to eq 9 in methanol according to a procedure described earlier.[14] The

$$\mathrm{Ni(sal)_2\times 2H_2O} + 2\ \mathrm{R\text{-}NH_2} \rightarrow \mathrm{Ni(H\text{-}R\text{-}sal)_2} + 4\mathrm{H_2O} \qquad (9)$$

complexes were characterized by elemental analysis (CHN), visible absorption spectra, and specific rotation (see Table 1). The abbreviations *R*-NiA_2 and *S*-NiA_2 are used for the complexes NiA_2 obtained according to eq 9 to indicate that the amine $R-NH_2$ applied has the *R*-configuration and *S*-configuration, respectively. Complexes NiB were prepared as reported.[12]

Instrumentation. UV/vis spectra, diode array spectrophotometer (Zeiss, type Specord S10). NIR spectra, double beam spectrophotometer (Perkin-Elmer, type Lambda 900). Specific rotation, polarimeter (Perkin-Elmer, type 241 and type 341). CD spectra, spectropolarimeter (Jasco, type J-720). Stopped-flow measurements, rapid scan stopped−flow spectrophotometer (J & M, type TIDAS),[15] operated with a manually driven syringes.

Kinetic Measurements. When slow enough, reaction (3) was followed by conventional spectrophotometry in two-chamber quartz cells (2 × 0.439 cm) and/or by conventional polarimetry in a polarimetric cuvette (1 dm). When faster ($t_{1/2}$ < 2 min), reaction (3) was studied by multiwavelength stopped-flow spectrophotometry in the wavelength range 400−620 nm. The (*A*,*t*) data (*A* = absorbance), as obtained under pseudo-first-order conditions ($[H_2B]_o > 0.1 \times [NiA_2]_o$), were computer-fitted to eq 10 or 11, whereas the (*A*,*t*) data and (*a*,*t*) data (α = specific rotation) obtained under stoichiometric conditions ($[H_2B]_o = [NiA_2]_o$) were fitted to eq 12 or 13, describing an irreversible second-order reaction (a_1, a_2 = amplitudes of the corresponding exponentials). The programs used were based on the least-squares method.

$$A = (A_o - A_\infty) \times [\exp(-k_{obsd} \times t)] + A_\infty \qquad (10)$$

$$A = a_1 \times [\exp(-k_{obsd(1)} \times t)] + a_2 \times [\exp(-k_{obsd(2)} \times t)] + A_\infty \qquad (11)$$

$$A = A_\infty + (A_o - A_\infty)/(1 + [\mathrm{complex}]_o \times k \times t) \qquad (12)$$

$$\alpha = \alpha_\infty + (\alpha_o - \alpha_\infty)/(1 + [\mathrm{complex}]_o \times k \times t) \qquad (13)$$

Results and Discussion

Properties of the Complexes and Ligands. In poorly coordinating solvents such as acetone, bis (*N*-alkylsalicylaldiminato nickel(II) complexes Ni(R-sal)$_2$ prefer to have a planar *trans*-N_2O_2 coordination geometry, which is documented by a strong CT band at 410−420 nm and a relatively weak d−d band at approximately 600 nm.[9,16] These two "planar" absorptions are indeed observed for complexes **1**, **3**, **4**, and **5** (see Table 1). The absorption of complexes **2** and **6** is subject to the substituent effect of the nitro group in that both bands are blue-shifted.

Complexes Ni(R-sal)$_2$ with α-branched alkyl groups R, such as in complexes **1**, **2**, and **4**, tend to establish a configurational equilibrium in solution, planar ⇌ tetrahedral.[16−18] The NIR absorption of complex **2** at 1075 nm is probably an indication of this equilibrium. It was shown, however, that, in ligand substitution reactions according to eq 3, the planar configurational isomer is the reacting one.[17,18]

The planar *cis*-N_2O_2 salen complexes Ni(*i*Busalen), Ni[(tBu)(Cl)*i*Busalen], and Ni(Bzsalen) have a characteristic absorption

(13) Warmuth, R. Dr.-Ing. Dissertation, Technische Hochschule Darmstadt, 1991.
(14) Schumann, M.; von Holtum, A.; Wannowius, K. J.; Elias, H. *Inorg. Chem.* **1982**, *21*, 606.
(15) Drexler, C.; Elias, H.; Fecher, B.; Wannowius, K. J. *Fresenius J. Anal. Chem.* **1991**, *340*, 605.
(16) Holm, R. H.; O'Connor, M. J. *Prog. Inorg.Chem.* **1971**, *14*, 241.
(17) Schumann, M.; Elias, H. *Inorg. Chem*. **1985**, *24*, 3187.
(18) Knoch, R.; Elias, H.; Paulus, H. *Inorg. Chem.* **1995**, *34*, 4032.

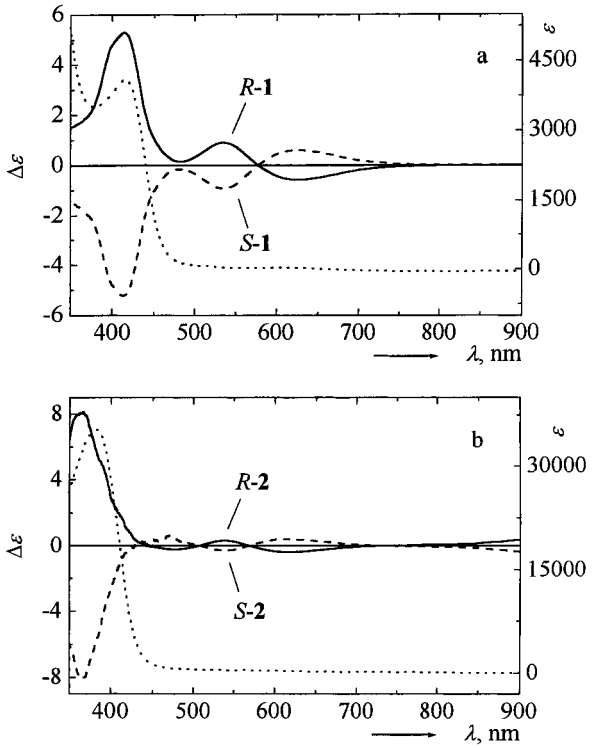

Figure 1. Absorption spectra of complexes **1** (a) and **2** (b) (dotted lines) and CD spectra of the enantiomers of complexes **1** (a) and **2** (b) in acetone at 298 K.

band in the range of 530−550 nm (see Table 1), which can be used for monitoring product formation according to reaction (3).

The optical purity of the enantiomers of the various complexes and ligands is confirmed by the data obtained for the specific rotation of the corresponding pairs of enantiomers, which agree within the limits of error (Table 1). The CD spectra of the complexes *R*-(+)-**1** and *R*-(+)-**2** are mirror-invertedly equal to the corresponding spectra of the enantiomers *S*-(−)-**1** and *S*-(−)-**2**, respectively (see Figure 1).

Kinetics of Ligand Substitution in Complexes 1 and 3−6 by Ligands II−IV. Under pseudo-first-order conditions ([complex] ≪ [entering ligand]), the (*A*,*t*) data obtained for reaction (3), studied spectrophotometrically with the various combinations of complexes **1**, **3**, **5,** and **6** and ligands **II**−**IV**, could be well fitted by eq 10, which led to experimental rate constant k_{obsd}. It was found that k_{obsd} increases linearly with the concentration of the entering ligand H_2B (see Figures S1-S18) according to $k_{obsd} = k \times [H_2B]$. This linear dependence yielded second-order rate constant *k* according to rate law (4). The data obtained for *k* are summarized in Table 2 and Table 3.

Mechanistically, the substitution of the two bidentate ligands HA in complexes NiA_2 by tetradentate ligands H_2B follows reaction sequence (5)−(7). The overall reaction is therefore expected to be biphasic with rate constants $k_{obsd(1)}$ and $k_{obsd(2)}$ and, under pseudo-first-order conditions, the concentration dependence of $k_{obsd(1)}$ should follow eq 14. It is found

$$k_{obsd(1)} = \frac{k_1 \cdot K \cdot [H_2B]}{1 + K \cdot [H_2B]} \qquad (14)$$

experimentally however that ligand substitution in complexes **1**, **3**, **5**, and **6** by ligands **II**−**IV** is properly described by second-order rate law (4). This means that, in the systems studied, the following two conditions, $k_2 \gg k_1$ and $K \times [H_2B] \ll 1$, are obviously fulfilled. These conditions make the overall reaction monophasic and let eq 14 take the simple form $k_{obsd(1)} = k_1 \times K \times [H_2B]$. The plot of $k_{obsd(1)}$ vs $[H_2B]$ thus yields a second-order rate constant *k* for reaction 3 which is a composite parameter according to $k = k_1 \times K$.

Table 2. Second-Order Rate Constant *k* ($M^{-1}s^{-1}$) for the Reaction of the Enantiomers of Complexes **1** and **3**−**6** with the Enantiomers of Ligand **II** in Acetone at 298 K According to Eq 3[a]

	ligand **II**		
	k		
complex	*R*	*S*	ratio[b]
R-**1**	59.5 ± 6.0	28.1 ± 2.8	2.1
	55.6 ± 5.6[c]	32.0 ± 3.2[c]	1.7
S-**1**	28.9 ± 2.9	54.8 ± 5.5	1.9
	30.7 ± 3.1[c]	59.2 ± 5.9[c]	1.9
R-**3**	9.1 ± 0.9	8.6 ± 0.9	1.1
	8.9 ± 0.9[c]	8.5 ± 0.9[c]	1.1
	9.4 ± 0.9[d]	8.8 ± 0.9[d]	1.1
S-**3**	8.7 ± 0.9	9.3 ± 0.9	1.1
	8.5 ± 0.9[c]	9.8 ± 1.0[c]	1.2
	8.7 ± 0.9[d]	10.1 ± 1.0[d]	1.2
R-**4**	1.5 ± 0.3[c]	2.6 ± 0.3[c]	1.7
	1.6 ± 0.2[d]	2.7 ± 0.3[d]	1.7
S-**4**	2.5 ± 0.3[c]	1.5 ± 0.2[c]	1.7
	2.6 ± 0.3[d]	1.5 ± 0.2[d]	1.7
5	0.0126 ± 0.0013[e]	0.0384 ± 0.0038[e]	3.0
6	2.0 ± 0.2[f]	2.1 ± 0.2[f]	1.1

[a] Experiments carried out under pseudo-first-order conditions ($[\mathbf{II}]_o > 0.1 \times [NiA_2]_o$) at five different concentrations of **II** in the range 0.002−0.032 M; rate constant k_{obsd} obtained by fitting the (*A*,*t*) data for the wavelength range 400−500 nm to eq 10, with rate constant *k* resulting from the plot of k_{obsd} vs [**II**]. [b] Ratio of rate constants, k_{fast}/k_{slow}, with k_{fast} being rate constant *k* for the faster reacting pair of enantiomers and vice versa. [c] Rate constant obtained under 1:1 conditions ($[NiA_2]_o = [\mathbf{II}]_o$) by fitting the (*A*,*t*) data to eq 12. [d] Rate constant obtained under stoichiometric conditions ($[NiA_2]_o = [\mathbf{II}]$) by fitting the *a*/*t* data to eq 13. [e] Experiments carried out at five different concentrations of **II** in the range $1.6 \times 10^{-3} - 0.025$ M. [f] Experiments carried out at five different concentrations of **II** in the range $3.1 \times 10^{-4} - 1.9 \times 10^{-3}$ M.

From the chemical point of view, these findings indicate that adduct formation between complexes **1**, **3**, **5**, and **6** and ligands **II**−**IV** is obviously too weak to make equilibrium (5) kinetically observable.

Stereoselectivity in Systems NiA_2/H_2B with NiA_2 = 1, 3−6 and H_2B = II. Table 2 summarizes the data obtained for rate constant *k* at 298 K by different methods (spectrophotometry and polarimetry) and under different conditions (excess of H_2B or concentration ratio 1:1; see Figures S28−S32 as examples). It is satisfying to see that the results obtained spectrophotometrically or polarimetrically and under excess or 1:1 conditions for a given combination of enantiomers agree well within the limits of error of approximately ± 10%. For systems **1**/**II**, **3**/**II**, and **4**/**II** both enantiomers of the complex and of the entering ligand were available which allowed to measure reaction (3) for all of the four combinations of enantiomers possible. The data clearly demonstrate the existence of chiral recognition in that there are "faster" and "slower" combinations of enantiomers for a given system. As an example, Figure 2 shows for the system **4**/**II** that the combination *R*-**4**/*S*-**II** is faster in ligand substitution than the combination *R*-**4**/*R*-**II**. The polarimetric data (Figure 2b) let this sort of chiral discrimination appear even more impressive than the spectrophotometric data (Figure 2a), but the corresponding rate constants (polarimetry: 2.7 and 1.6 $M^{-1}\,s^{-1}$; spectrophotometry: 2.6 and 1.5 $M^{-1}\,s^{-1}$) are of equal quality (see Table 2). It is important to note that the "mirror" combinations *S*-**4**/*R*-**II** and *S*-**4**/*S*-**II**, respectively, lead to the analogous result in that (for system **4**/**II**) the "mixed" *R*/*S*

Table 3. Second-Order Rate Constant k (M^{-1} s^{-1}) for the Reaction of the Enantiomers of Complex **1** with the Enantiomers of Ligands **II**−**IV** in Acetone at 298 K According to Eq 3[a]

	ligand **II**			ligand **III**			ligand **IV**		
	k			k			k		
complex	*R*	*S*	ratio[b]	*R*	*S*	ratio[b]	*R*	*S*	ratio[b]
R-**1**	59.5 ± 6.0	28.1 ± 2.8	2.1	7.1 ± 0.7	7.1 ± 0.7	1.0	67.1 ± 6.7	46.6 ± 4.7	1.4
S-**1**	28.9 ± 2.9	54.8 ± 5.5	2.0				43.6 ± 4.4	67.3 ± 6.7	1.5

[a] Experiments carried out under pseudo-first-order conditions ($[\text{ligand}]_o > 0.1\times[\mathbf{1}]_o$) at five different concentrations of ligand **II**−**IV** in the range from 0.002 to 0.032 M; rate constant k_{obsd} obtained by fitting the (A,t) data to eq 10, with rate constant k resulting from the plot of k_{obsd} vs [ligand H_2B]. [b] Ratio of rate constants, k_{fast}/k_{slow}, with k_{fast} being rate constant k for the faster reacting pair of enantiomers and vice versa.

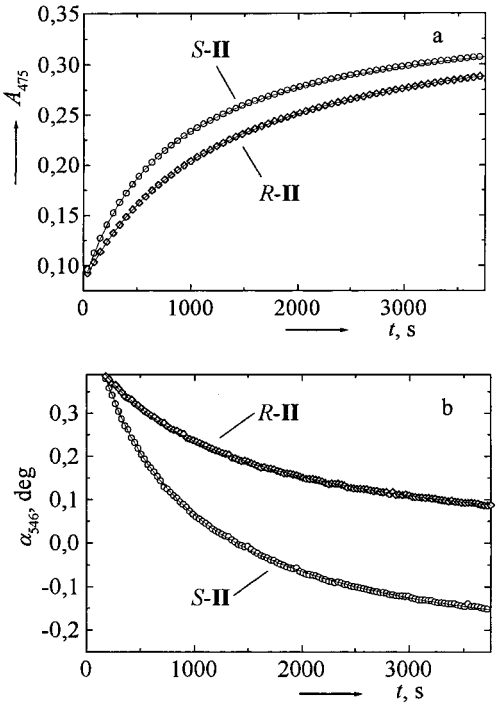

Figure 2. Plot of absorbance A (a) and specific rotation α (b) vs time for the reactions of complex *R*-**4** with ligands *R*-**II** and *S*-**II**, respectively, in acetone at 298 K ($[R\text{-}\mathbf{4}] = [\mathbf{II}] = 5 \times 10^{-4}$ M; the solid lines are fitting curves according to eq 12 and eq 13, respectively).

combination is faster than the *S*/*S* (or *R*/*R)* combination. As a measure for chiral recognition in system **4**/**II**, the ratio of rate constants k representing the "faster" and "slower" combination of enantiomers is found to be 1.7 (Table 2).

From the chemical point of view, the difference between complexes **4** and **1** is that, in **1**, the 1-naphthyl group in **4** has been replaced by a phenyl group (see Chart 1). For system **1**/**II**, as studied spectrophotometrically with all of the four combinations of enantiomers, the ratio of "fast" and "slow" rate constants ranges from 1.7 to 2.1 with a mean of 1.9. This means that, depending on the chirality of the partners, for this system the rate of reaction (3) can differ by a factor of almost two. One should note that, in contrast to system **4**/**II**, here the "faster" combination of enantiomers is the *R*/*R* and *S*/*S* combination with the "mixed" *R*/*S* combination being the slower one.

The difference between complexes **1** and **3** is that, in **3**, the chiral carbon atom has been shifted away from the central nickel by the insertion of a methylene group, acting as a "spacer" (see Chart 1). The kinetic effect of this is that the rate of ligand substitution drops and chiral recognition is lost almost completely, the average discrimination ratio being only 1.15 (see Table 2).

The introduction of the bulky dehydroabietyl group with three chiral carbon atoms in complex **5** reduces the rate of ligand substitution by *R*-**II** and *S*-**II** considerably. On the other hand, the phenomenon of chiral discrimination is very pronounced. To our knowledge, the ratio $k_{fast}/k_{slow} = 3.0$ obtained for this system represents the highest stereoselectivity reported so far for ligand substitution in nickel(II) complexes with pairs of enantiomers as reaction partners. Interestingly, the introduction of the electron-withdrawing nitro group in complex **6** raises the reaction rate substantially and lets the extent of chiral recognition diminish to $k_{fast}/k_{slow} = 1.1$ (Table 2). In a comparable system, Jacobsen et al. observed the same phenomenon, namely, increased rate and reduced stereoselectivity upon introduction of nitro substituents.[3c]

In conclusion, the rate data compiled in Table 2 reflect clearly that the extent of chiral recognition associated with reaction (3) is strongly affected by the nature of the chiral group R attached to the imine nitrogen atom in complexes NiA_2.

Stereoselectivity in Systems NiA_2/H_2B with NiA_2 = 1 and H_2B = II−IV. Table 3 summarizes the rate data obtained for reaction (3), as studied with complex **1** and three ligands H_2B differing in the nature of the group R′ (see Chart 1). As found for the variation of group R in complexes NiA_2 (see Table 2), the variation of group R′ attached to the chiral carbon atom of the ethylene bridge in the salen ligands **II** and **IV** affects the extent of chiral discrimination markedly. The mean of ratio k_{fast}/k_{slow} ranges from 1.45 (**IV**) to 2.05 (**II**), with $k_{fast}/k_{slow} = 1.7$ for ligand **I**[9] lying between. Bulky substituents in combination with electron-withdrawing substituents on the phenyl rings as in ligand **III** (X = *tert*-butyl, Y = Cl; see Chart 1) let the mean ratio k_{fast}/k_{slow} drop from 2.05 (**II**) to 1.0. To explain the complete disappearance of chiral recognition upon going from system **1**/**II** to system **1**/**III** one might argue that the bulky *tert*-butyl groups dominate the stereochemistry of adduct formation so much that the chiral information, located on the ethylene bridge of **III**, does not have an effect.

Ligand Substitution in System 2/II: Biphasic Kinetics and Activation Parameters. It is well-known that planar *trans*-N_2O_2 complexes NiA_2 tend to expand their coordinaton number, forming five- and preferably six-coordinate species.[19] As shown by spectrophotometric titration with bases B according to eq 15, equilibrium constant K_B for a given complex NiA_2 and base

$$NiA_2 + B \overset{K_B}{\rightleftharpoons} NiA_2{\cdot}B \qquad (15)$$

B increases drastically when nitro substituents are introduced in NiA_2.[10] Due to the electron-withdrawing effect of the nitro group, the Lewis acidity of the nickel center is obviously increased. It is therefore to be expected that, compared to complex **1**, adduct formation with nitro-substituted complex **2** according to eq 5 will be favored.

The investigation of reaction (3) with complex **2** and entering ligand **II** shows that ligand substitution is no longer monophasic

(19) See refs 9, 14, and 17 and the literature cited therein.

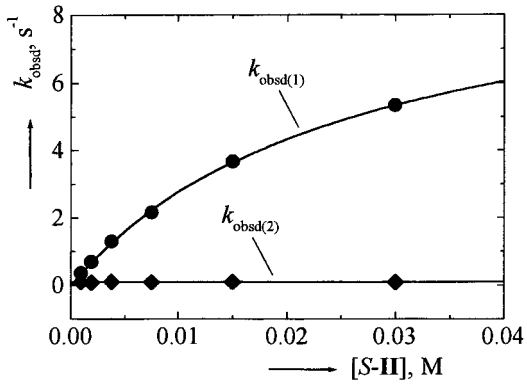

Figure 3. Plot of experimental rate constants $k_{obsd(1)}$ and $k_{obsd(2)}$ vs concentration of the entering ligand *S*-**II** for complex *R*-**2** reacting according to eq 3 in acetone at 298 K (the solid line connecting the $k_{obsd(1)}$ data is the fitting curve according to eq 14).

Table 4. Summary of Rate and Equilibrium Data for Reaction 3 Studied with Complex **2** and Ligand **II** in Acetone at 298 K[a]

complex **2**	ligand **II**	K, M^{-1} [b]	k_1, s^{-1} [b]	$k = K \times k_1$, $M^{-1}\,s^{-1}$	ratio (k)[c]	k_2, s^{-1} [f]
R	*R*	34.9 ± 1.9	12.2 ± 0.4	426 ± 28	1.1	0.094 ± 0.003
R	*S*	38.3 ± 2.0	10.0 ± 0.3	383 ± 23		0.094 ± 0.004
S	*R*	44.7 ± 3.0	9.6 ± 0.3	429 ± 32	1.1	0.097 ± 0.003
S	*S*	30.3 ± 2.8	12.6 ± 0.7	382 ± 42		0.098 ± 0.005

[a] Experiments carried out under pseudo-first-order conditions ($[\mathbf{II}]_o > 0.1\times[\mathbf{2}]_o$) at six different concentrations of **II** in the range $9.4\times10^{-4} - 0.03$ M; rate constants $k_{obsd(1)}$ and $k_{obsd(2)}$ obtained by fitting the (A,t) data to eq 11. [b] As obtained from the dependence $k_{obsd(1)} = f([\mathbf{II}]_o)$ according to eq 14; limits of error obtained upon least-squares fitting of the data. [c] Ratio$(k) = k_{fast}/k_{slow}$, with k_{fast} being rate constant k for the faster reacting pair of enantiomers and *vice versa*. [df] From the equivalence $k_{obsd(2)} = k_2$ according to reaction sequence (5)−(7).

(as it is in the case of complex **1**) but biphasic, as expected according to reaction sequence (5)−(7). The (A,t) data obtained can be well fitted to eq 11 which leads to first-order rate constants $k_{obsd(1)}$ and $k_{obsd(2)}$. As shown in Figure 3 for the enantiomer combination *R*-**2**/*S*-**II**, $k_{obsd(1)}$ depends on the concentration of the excess partner *S*-**II**, whereas $k_{obsd(2)}$ is independent of [*S*-**II**] (see also Figures S19−S24). Fitting of the $k_{obsd(1)}$ data to eq 14 yields equilibrium constant K and rate constant k_1, with $k_{obsd(2)}$ corresponding to rate constant k_2 according to eqs 5−7 (see Table 4). System **2**/**II** is therefore a most interesting system as it allows the separation of thermodynamic and kinetic parameters.

One has to consider that, as shown schematically in Scheme 1, the overall process of ligand substitution according to (3) is associated with considerable stereochemical changes (HO∩N = bidentate ligand HA; HO∩N∩N∩OH = tetradentate salen ligand H_2B). One of the two bidentate N,O ligands in NiA_2 has to be bent out of the NiN_2O_2 coordination plane to provide two neighboring sites for the N,N coordination of the salen ligand H_2B in the adduct with a (distorted) octahedral coordination.[20] Fast adduct formation is followed by elimination of the first bidentate ligand with first-order rate constant k_1, which necessitates intramolecular proton transfer and additional steric rearrangement. The k_1 step leads to an intermediate the spectroscopic characterization of which is hampered by the absorption of ligand **II** present in excess. In Scheme 1, we suggest a quasi-octahedral donor atom arrangement for the intermediate with the second phenolic OH group of H_2B loosely attached to the nickel. In the last step with first-order rate constant k_2 internal proton transfer and final ligand rearrangement leads to planar NiB.

The results obtained from the temperature dependence of ligand substitution in system *S*-**2**/*R*-**II** are presented in Table 5 (see also Table S1 and Figures S25−S27). Adduct formation is an exothermic process ($\Delta H° = -18$ kJ mol^{-1}). The activation barriers for the dissociation of the two bidentate ligands, as characterized by $\Delta H^{\neq} = 50$ kJ mol^{-1} for the k_1 step and $\Delta H^{\neq} = 37$ kJ mol^{-1} for the k_2 step, refer to intramolecular concerted processes consisting of proton transfer, bond making, and release of a bidentate ligand. It is interesting to note that (i) the entropy of activation for both the k_1 step and the k_2 step is clearly negative and (ii) the experimental finding, $k_1 > k_2$, is based on a higher enthalpy of activation and smaller negative entropy of activation for the faster k_1 step and vice versa for the slower k_2 step. These results might indicate that differences between the state of solvation of the more or less octahedral adduct and intermediate and the state of solvation of the planar product NiB play an important role.

Stereoselectivity in System 2/II. Reaction (3) was studied with all of the four possible combinations of enantiomers of **2** and **II** (see experimental data in Figure 3 and Figures S19−S21). The final results obtained for K, k_1, and k_2 as well as for the (calculated) parameter $k_1\times K$ are summarized in Table 4. It is found that rate constant k_1, describing the dissociation of the first bidentate ligand HA from the adduct **2**×**II**, is higher for the combinations *R*-**2**/*R*-**II** and *S*-**2**/*S*-**II** compared to the "mixed" combinations *R*-**2**/*S*-**II** and *S*-**2**/*R*-**II**. The data obtained for equilibrium constant K, describing adduct formation between **2** and **II**, follow the same, but mirror-inverted trend. K is smaller for the combinations *R*-**2**/*R*-**II** and *S*-**2**/*S*-**II** compared to the combinations *R*-**2**/*S*-**II** and *S*-**2**/*R*-**II**. In other words, dissociation from the less stable adduct **2**×**II** is faster and vice versa. These results correspond to the "major/minor" principle, as suggested by Halpern and co-workers[4] (see Introduction). For the (calculated) product $K\times k_1$ (= k) the higher (lower) rate compensates the lower (higher) stability and the parameter ratio(k) is found to be 1.1 only (see Table 4).

The extent of chiral discrimination observed for ligand substitution in system **2**/**II** is small. The corresponding differences in equilibrium constant K and rate constant k_1 have to be critically compared to the limits of error, as resulting from the fitting procedure according to eq 14. The limits of error for k_1 and K are of the order of 3−5% and 5−9%, respectively. The differences in k_1 and K for the various combinations of enantiomers are found to lie out of these limits of error, but they are close to them. One has to admit therefore that the chiral discrimination observed for system **2**/**II** is too small to allow a detailed discussion as to whether the stereoselectivity originates from adduct formation (K) and/or ligand dissociation (k_1). It follows from the data obtained for rate constant k_2 that dissociation of the second bidentate ligand is not subject to chiral discrimination.

(20) In an earlier study[10] we provided convincing spectroscopic evidence that, in the adducts formed from *N*-alkylsalicylaldiminato nickel(II) complexes, NiA_2, and salen-type ligands, H_2B, the tetradentate N_2O_2 ligand H_2B is *cis*-*N*,*N* coordinated. One has to consider that, for adducts $NiA_2\times H_2B$ with an octahedral $(N,N)(N,O)_2$ coordination core, three (chiral) stereoisomers can be envisaged. The *cis*-N_2-*trans*-O_2 mode of coordination, suggested in Scheme 1 for the two bidentate N,O ligands of the adduct, was chosen in view of the corresponding stereochemisty of the octahedral adduct $Ni(Et\text{-}sal)_2\times bpy$, as determined by X-ray crystallography.[21]

(21) Viehmann, N.; Dr.-Ing. Dissertation, Technische Hochschule Darmstadt, 1993.

Scheme 1. Stereochemical Changes Associated with Reaction (3)

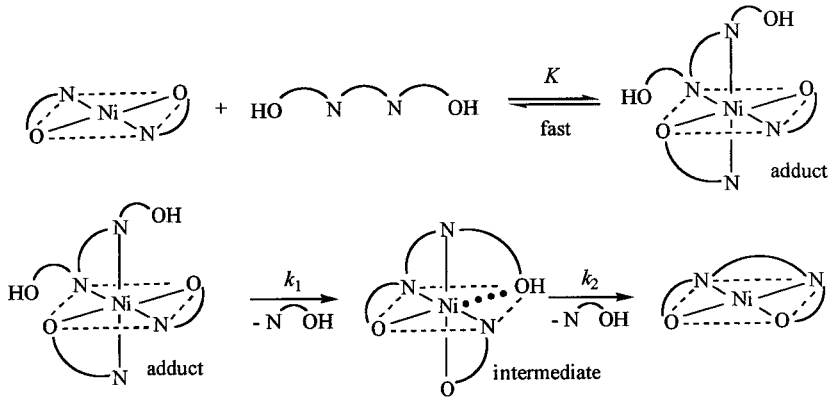

Table 5. Activation Parameters and Thermodynamic Parameters for Ligand Substitution According to Reaction (3) as Studied with the Complex *S*-**2** and Ligand *R*-**II** in Acetone

reaction step	$\Delta H^{\neq}$/kJ mol^{-1}	$\Delta S^{\neq}$/J mol^{-1} K^{-1}	reaction step	$\Delta H°$/kJ mol^{-1}	$\Delta S°$/J mol^{-1} K^{-1}
rate-controlling loss of the first bidentate ligand with rate constant k_1 (see eq 6)	50 ± 1^a	-57 ± 4^a	adduct formation with equilibrium constant K (see eq 5)	-18 ± 2^c	-29 ± 7^c
consecutive loss of the second bidentate ligand with rate constant k_2 (see eq 7)	37 ± 5^b	-140 ± 39^b			

[a] From the temperature dependence of k_1 determined at four temperatures in the range 288−303 K. [b] From the temperature dependence of k_2 determined at four temperatures in the range 288−303 K. [c] From the temperature dependence of K, as obtained at four temperatures in the range 288−303 K according to $\ln K = -\Delta H°/(RT) + \Delta S°/R$.

Summary of Main Results

Ligand substitution in bis *N*-alkylsalicylaldiminato nickel(II) complexes NiA_2 by salen-type ligands H_2B according to reaction (a) is an associatively controlled process, following

$$NiA_2 + H_2B \xrightarrow{k} NiB + 2HA \quad \text{(a)}$$

$$NiA_2 + H_2B \overset{K}{\rightleftharpoons} \{NiA_2,H_2B\} \xrightarrow{k_1} NiAHB + HA \xrightarrow{k_2} NiB + 2HA \quad \text{(b)}$$

reaction sequence (b). In most cases reaction (a) is found to be a monophasic second-order process, rate $= k\times[NiA_2]\times[H_2B]$, with $k = k_1 \times K$.

Substitution reaction (a), when studied with the various enantiomers of chiral complexes NiA_2 and chiral ligands H_2B, is found to be subject to chiral discrimination. The ratio of second-order rate constants, k_{fast}/k_{slow}, with k_{fast} being rate constant k for the faster reacting pair of enantiomers and vice versa, lies in the range 1.0−3.0, depending on the nature of chirality center in NiA_2 and H_2B.

For one of the chiral systems NiA_2/H_2B, biphasic kinetics according to reaction sequence (b) are observed and the data for equilibrium constant K and rate constants k_1 and k_2 are available for the various pairs of enantiomers. In this system the extent of stereoselectivity is unfortunately rather limited and the data do not allow reliable conclusions concerning the thermodynamic (K) or kinetic (k) origin of chiral discrimination.

Acknowledgment. Sponsorship of this work by the Deutsche Forschungsgemeinschaft and Verband der Chemischen Industrie e.V. is gratefully acknowledged. The authors thank Dr. K. Beckenkamp (Merck, Darmstadt) for the possibility to do some polarimetric measurements in his laboratory.

Supporting Information Available: Seven pages with Figures S1−S32 and Table S1 presenting the concentration dependence and temperature dependence of the experimental rate constants. This material is available free of charge via the Internet at http://pubs.acs.org.

IC000339M